

## ON THE RELATION BETWEEN CIRCULAR VELOCITY AND CENTRAL VELOCITY DISPERSION IN HIGH AND LOW SURFACE BRIGHTNESS GALAXIES<sup>1</sup>

A. PIZZELLA,<sup>2</sup> E. M. CORSINI,<sup>2</sup> E. DALLA BONTÀ,<sup>2</sup> M. SARZI,<sup>3</sup> L. COCCATO,<sup>2</sup> AND F. BERTOLA<sup>2</sup>

Received 2005 January 5; accepted 2005 March 24

### ABSTRACT

In order to investigate the correlation between the circular velocity  $V_c$  and the central velocity dispersion of the spheroidal component  $\sigma_c$ , we analyzed these quantities for a sample of 40 high surface brightness (HSB) disk galaxies, eight giant low surface brightness (LSB) spiral galaxies, and 24 elliptical galaxies characterized by flat rotation curves. Galaxies have been selected to have a velocity gradient  $\leq 2 \text{ km s}^{-1} \text{ kpc}^{-1}$  for  $R \geq 0.35R_{25}$ . We used these data to better define the previous  $V_c$ - $\sigma_c$  correlation for spiral galaxies (which turned out to be HSB) and elliptical galaxies, especially at the lower end of the  $\sigma_c$  values. We find that the  $V_c$ - $\sigma_c$  relation is described by a linear law out to velocity dispersions as low as  $\sigma_c \approx 50 \text{ km s}^{-1}$ , while in previous works a power law was adopted for galaxies with  $\sigma_c > 80 \text{ km s}^{-1}$ . Elliptical galaxies with  $V_c$  based on dynamical models or directly derived from the H I rotation curves follow the same relation as the HSB galaxies in the  $V_c$ - $\sigma_c$  plane. On the other hand, the LSB galaxies follow a different relation, since most of them show either higher  $V_c$  or lower  $\sigma_c$  with respect to the HSB galaxies. This argues against the relevance of baryon collapse to the radial density profile of the dark matter halos of LSB galaxies. Moreover, if the  $V_c$ - $\sigma_c$  relation is equivalent to one between the mass of the dark matter halo and that of the supermassive black hole, then these results suggest that the LSB galaxies host a supermassive black hole (SMBH) with a smaller mass compared to HSB galaxies with an equal dark matter halo. On the other hand, if the fundamental correlation of SMBH mass is with the halo circular velocity, then LSB galaxies should have larger black hole masses for a given bulge dispersion. Elliptical galaxies with  $V_c$  derived from H I data and LSB galaxies were not considered in previous studies.

*Subject headings:* black hole physics — galaxies: elliptical and lenticular, cD —  
galaxies: fundamental parameters — galaxies: halos —  
galaxies: kinematics and dynamics — galaxies: spiral

*Online material:* color figure

### 1. INTRODUCTION

A possible relation between the central velocity dispersion of the spheroidal component ( $\sigma_c$ ) and the galaxy circular velocity measured in the flat region of the rotation curve ( $V_c$ ) was suggested by Whitmore et al. (1979) and Whitmore & Kirshner (1981). By measuring H I line widths, they found that  $V_c/\sigma_c \sim 1.7$  for a sample of S0 and spiral galaxies. Recently, Ferrarese (2002) proceeded further, extending the  $V_c$ - $\sigma_c$  relation to elliptical galaxies. She interpreted the  $V_c$ - $\sigma_c$  relation as suggestive of a correlation between two different galactic components, since  $\sigma_c$  and  $V_c$  probe the potential of the spheroidal component and of the dark matter (DM) halo, respectively. In particular, it results that for a given DM halo the central velocity dispersion of the spheroidal component is independent of the morphological type. The validity of this relation has been confirmed by Baes et al. (2003), who enlarged the sample of spiral galaxies.

For elliptical galaxies,  $V_c$  is generally inferred by means of dynamical modeling of the stellar kinematics. This is the case for the giant round and almost nonrotating elliptical galaxies studied by Kronawitter et al. (2000). These galaxies form a unique dynamical family that scales with luminosity and ef-

fective radius. As a consequence, the maximum circular velocity is correlated with the central velocity dispersion of the galaxy (Gerhard et al. 2001). Whether the same is true for more flattened and fainter elliptical galaxies is still to be investigated. On the other hand, both the shape and amplitude of the rotation curve of a spiral galaxy depend on the galaxy luminosity and morphological type (e.g., Burstein & Rubin 1985; Persic et al. 1996). For this reason, for spiral galaxies the  $V_c$ - $\sigma_c$  relation is not expected a priori.

It is interesting to investigate whether the  $V_c$ - $\sigma_c$  relation also holds for less dense objects characterized by a less steep potential well. This is the case for low surface brightness (LSB) galaxies, which are disk galaxies with a central face-on surface brightness  $\mu_B \geq 22.6 \text{ mag arcsec}^{-2}$  (e.g., Schombert et al. 1992; Impey et al. 1996). Previous work concentrated on high surface brightness (HSB) galaxies, and to infer the  $V_c$  for elliptical galaxies, they relied on stellar dynamical models. In this work we investigate the behavior of elliptical galaxies with H I-based  $V_c$  and of LSB galaxies in the  $V_c$ - $\sigma_c$  relation.

This paper is organized as follows. An overview of the properties of the sample galaxies, as well as an analysis of the kinematic data available in the literature to derive their  $V_c$  and  $\sigma_c$ , are presented in § 2. The results and discussion concerning the  $V_c$ - $\sigma_c$  relation are given in § 3.

### 2. SAMPLE SELECTION

In the past years we started a scientific program aimed at deriving the detailed kinematics of ionized gas and stars in HSB and LSB galaxies in order to study their mass distributions and

<sup>1</sup> Based on observations made with European Southern Observatory telescopes at the Paranal Observatory under programs 67.B-0283, 69.B-0573, and 70.B-0171.

<sup>2</sup> Dipartimento di Astronomia, Università di Padova, vicolo dell'Osservatorio 2, I-35122 Padova, Italy.

<sup>3</sup> Physics Department, University of Oxford, Keble Road, Oxford OX1 3RH, UK.

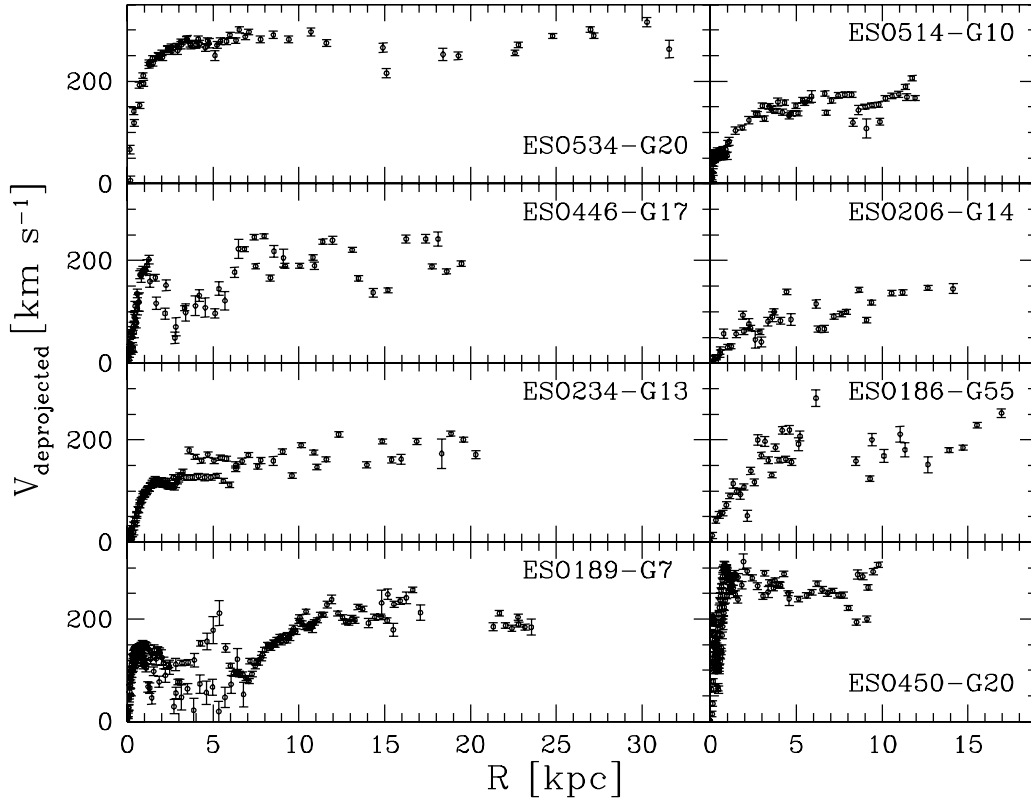


FIG. 1.—Deprojected rotation curves of the eight LSB galaxies of the final sample.

structural properties. We measured the velocity curves and velocity dispersion profiles along the major axis for both the ionized-gas and stellar components for a preliminary sample of 50 HSB galaxies (10 S0–S0/a galaxies in Corsini et al. [2003]; seven Sa galaxies in Bertola et al. [1996] and Corsini et al. [1999]; 16 S0–Sc galaxies in Vega Beltrán et al. [2001]; and 17 Sb–Scd galaxies in Pizzella et al. [2004b]) and 11 LSB galaxies (A. Pizzella et al. 2005, in preparation; Pizzella et al. 2004a).

The HSB sample consists of disk galaxies with Hubble type ranging from S0 to Scd, an inclination  $i \geq 30^\circ$ , and a distance  $D < 80$  Mpc. The LSB sample consists of disk galaxies with Hubble type ranging from Sa to Irr, an intermediate inclination ( $30^\circ \lesssim i < 70^\circ$ ), and a distance  $D < 65$  Mpc (except for ESO 534-G20). Three LSB galaxies, namely, ESO 206-G14, ESO 488-G49, and LSBC F563-V02, have been selected from the sample observed by de Blok & McGaugh (1997). The remaining eight objects are LSB galaxies with bulge. They have been selected in Lauberts & Valentijn (1989, hereafter ESO-LV) to have a LSB disk component following the criteria described by Beijersbergen et al. (1999). Due to the bulge light contribution, the total central face-on surface brightness of the galaxy could be  $\mu_B \leq 22.6$  mag arcsec $^{-2}$ . However, all these objects do have a LSB disk. As far as their total luminosity is concerned, LSBC F563-V02 and ESO 488-G49 are two dwarf LSB galaxies, but the other nine objects are representative of giant LSB galaxies (e.g., McGaugh et al. 2001).

For all the HSB and LSB galaxies, we obtained the ionized-gas rotation curve by folding the observed line-of-sight velocities around the galaxy center and systemic velocity after averaging the contiguous data points and applying a correction for galaxy inclination. We rejected 35 HSB galaxies because they had asymmetric rotation curves or rotation curves

that were not characterized by an outer flat portion. Ferrarese (2002) and Baes et al. (2003) considered galaxies with the rotation curve extending farther out than  $R_{25}$ . This criterion is not appropriate when the sample of galaxies spans a wide range in photometric properties. For LSB galaxies, which have a lower central surface brightness than HSB galaxies,  $R_{25}$  corresponds to a relatively small radius, where the rotation curve may be still rising. For this reason we adopt a criterion that selects rotation curves on the basis of their flatness rather than on their extension.

The flatness of each rotation curve has been checked by fitting it with a linear law,  $V(R) = AR + B$  for  $R \geq 0.35R_{25}$ . The radial range has been chosen in order to avoid the bulge-dominated region of the rotation curve (e.g., IC 724 and NGC 2815). The rotation curves with  $|A| \geq 2$  km s $^{-1}$  kpc $^{-1}$  within  $3\sigma$  have been considered not to be flat. In this way 15 HSB galaxies and eight LSB galaxies resulted as having a flat rotation curve. Since the velocity curves of the LSB galaxies were not presented in previous papers, we show their folded rotation curves in Figure 1. We derived  $V_c$  by averaging the outermost values of the flat portion of the rotation curve.

We are therefore confident that we are giving a reliable estimate of the asymptotic value of the circular velocity that traces the mass of the DM halo (for a discussion, see Ferrarese 2002). We derived  $\sigma_c$  from the stellar kinematics by extrapolating the velocity dispersion radial profile to  $r = 0''$ . This has been done by fitting the eight innermost data points with an empirical function (either an exponential, a Gaussian, or a constant). We did not apply any aperture correction to  $\sigma_c$ , as discussed by Baes et al. (2003) and Pizzella et al. (2004b).

In order to complete our sample of disk galaxies, we included all the spiral galaxies previously studied by Ferrarese (2002) and Baes et al. (2003) that are in addition characterized by a flat

TABLE 1  
GALAXY SAMPLE

Name (1)	Morphological Type (2)	$i$ (deg) (3)	$D$ (Mpc) (4)	$M_{B_r}^0$ (mag) (5)	$\sigma_c$ (km s <sup>-1</sup> ) (6)	$V_c$ (km s <sup>-1</sup> ) (7)	$R_{\text{last}}$ ( $R_{25}$ ) (8)	References (9)
HSB Galaxies								
ESO 323-G25 .....	(R')SBbc(s):	55	59.8	-21.2	139 ± 14	228 ± 15	1.2	1
ESO 382-G58 .....	SBbc(r): sp	79	106.2	-22.2	165 ± 22	315 ± 20	1.1	1
ESO 383-G02 .....	SABc(rs)	60	85.4	-21.1	109 ± 28	190 ± 14	1.0	1
ESO 383-G88 .....	SABbc(r)?	67	59.5	-20.6	70 ± 14	177 ± 16	1.0	1
ESO 445-G15 .....	Sbc	66	60.3	-20.2	113 ± 13	190 ± 21	1.1	1
ESO 446-G01 .....	SAbc(s):	53	98.3	-21.4	123 ± 12	213 ± 17	1.0	1
ESO 501-G68 .....	Sbc	70	45.8	-20.1	100 ± 16	173.0 ± 9.0	1.1	1
IC 342 .....	SABcd(rs)	12	2.0	-20.5	77 ± 12	185 ± 10	1.4	2
IC 724 .....	Sa	55	78.0	-21.6	207.0 ± 2.8	284 ± 24	0.8	3
NGC 753 .....	SABbc(rs)	39	90.0	-22.4	121 ± 17	210.0 ± 7.0	0.6	2
NGC 801 .....	Sc	79	79.2	-21.9	144 ± 27	216.0 ± 9.0	1.6	2
NGC 1160 .....	Scd:	62	36.6	-21.0	25 ± 13	155.1 ± 4.0	0.8	4
NGC 1357 .....	SAab(s)	47	26.2	-20.0	121 ± 14	259.0 ± 5.0	0.8	2
NGC 1620 .....	SABbc(rs)	71	46.1	-21.1	92.2 ± 6.9	227.5 ± 4.7	1.1	5
NGC 2179 .....	SA0/a(s)	47	35.6	-19.9	175.6 ± 6.5	241 ± 11	1.0	3
NGC 2590 .....	SAbc(s):	72	63.4	-21.0	196 ± 16	259 ± 18	1.0	5
NGC 2639 .....	(R)SAa(r)?	53	66.5	-21.9	195 ± 13	318.0 ± 4.0	0.7	2
NGC 2815 .....	SBb(r):	72	40.0	-21.6	205.9 ± 9.8	270.7 ± 5.8	0.9	5
NGC 2844 .....	SAa(r):	61	26.4	-18.9	113 ± 12	171 ± 10	1.0	2
NGC 2998 .....	SABc(rs)	63	67.4	-21.6	113 ± 30	198.0 ± 5.0	1.7	2
NGC 3054 .....	SABb(r)	52	28.5	-20.3	138 ± 13	244.5 ± 3.3	0.9	5
NGC 3038 .....	SAb(rs)	58	41.4	-21.5	160 ± 16	256 ± 22	1.3	1
NGC 3145 .....	SBbc(rs)	60	61.0	-22.1	166 ± 12	261.0 ± 3.0	0.8	2
NGC 3198 .....	SBc(rs)	68	9.4	-19.7	69 ± 13	150.0 ± 3.0	5.2	2
NGC 3200 .....	SABc(rs):	73	43.4	-21.5	191.9 ± 3.9	272 ± 12	0.9	5
NGC 3223 .....	SAb(s)	53	46.5	-22.4	163 ± 17	261 ± 11	0.8	2
NGC 3333 .....	SABbc pec sp	82	59.4	-21.3	111 ± 23	208 ± 12	1.0	1
NGC 3885 .....	SA0/a(s)	67	22.3	-19.4	124.5 ± 7.5	156 ± 27	0.6	6
NGC 4378 .....	(R)SAa(s)	21	43.1	-21.0	198 ± 18	308.0 ± 1.0	0.5	2
NGC 4419 .....	SBa(s) sp	71	17.0	-19.6	99 ± 16	172.7 ± 4.5	0.4	4
NGC 4845 .....	SAab(s) sp	76	13.1	-19.2	80.6 ± 2.1	136 ± 17	0.5	3
NGC 5055 .....	SAbc(rs)	55	8.0	-20.5	103.0 ± 6.0	180.0 ± 5.0	2.4	2
NGC 5064 .....	(R')SAab:	63	36.0	-21.1	188.3 ± 4.6	272.9 ± 2.8	0.9	4
NGC 6503 .....	SAc(s)	71	5.9	-18.7	48 ± 10	116.0 ± 2.0	1.9	2
NGC 6925 .....	SAbc(s)	75	37.7	-21.9	190.0 ± 4.5	261.5 ± 9.1	1.0	5
NGC 7083 .....	SAbc(s)	53	39.7	-21.5	100.8 ± 4.4	235 ± 14	0.9	5
NGC 7217 .....	(R)SAab(r)	34	21.9	-21.2	171 ± 17	241.0 ± 4.0	0.7	2
NGC 7331 .....	SAb(s)	70	14.9	-21.5	139 ± 14	239.0 ± 5.0	1.6	2
NGC 7531 .....	SABbc(r)	67	20.9	-20.2	108.7 ± 5.6	168.6 ± 8.4	0.7	5
NGC 7606 .....	SAb(s)	67	42.1	-22.2	124 ± 21	240.0 ± 4.0	0.9	2
LSB Galaxies								
ESO 186-G55 .....	Sab(r)?	63	60.1	-19.1	91.7 ± 2.0	235 ± 11	1.0	7
ESO 189-G07 .....	SABbc(rs)	49	37.5	-20.2	91.3 ± 2.0	185.9 ± 6.9	1.0	7
ESO 206-G14 .....	SABc(s)	39	60.5	-19.0	54.3 ± 2.0	141.0 ± 4.5	1.4	7
ESO 234-G13 .....	Sbc	69	60.9	-19.3	64.1 ± 2.0	194 ± 19	1.2	7
ESO 446-G17 .....	(R)SBb(s)	54	58.9	-20.3	133.6 ± 2.0	196 ± 33	1.2	7
ESO 450-G20 .....	SBbc(s):	30	31.6	-19.5	112.4 ± 2.4	245 ± 35	1.0	7
ESO 514-G10 .....	SABc(s):	36	40.4	-20.2	60.2 ± 4.0	181 ± 15	0.8	7
ESO 534-G20 .....	Sa:	46	226.7	-20.7	153.9 ± 7.1	297 ± 11	1.4	7
Elliptical Galaxies with $V_c$ from H I Data								
IC 2006 .....	(R)SA0 <sup>-</sup>	31	16.7	-18.9	128.0 ± 1.7	221 ± 14	2.4	8, 9
NGC 2865 .....	E3-4	65	31.2	-20.3	169.4 ± 7.0	240 ± 15	3.2	10, 11
NGC 2974 .....	E4	55	24.0	-20.2	254.8 ± 3.8	355 ± 60	1.8	12, 8
NGC 4278 .....	E1-2	45	7.9	-18.5	250.7 ± 7.7	326 ± 40	3.3	13, 14
NGC 5266 .....	SA0 <sup>-</sup> :	63	37.1	-21.4	182.1 ± 9.3	270 ± 40	7.6	15, 16

TABLE 1—*Continued*

Name (1)	Morphological Type (2)	$i$ (deg) (3)	$D$ (Mpc) (4)	$M_{B_T}^0$ (mag) (5)	$\sigma_c$ (km s <sup>-1</sup> ) (6)	$V_c$ (km s <sup>-1</sup> ) (7)	$R_{\text{last}}$ ( $R_{25}$ ) (8)	References (9)
Elliptical Galaxies with $V_c$ from Dynamical Models								
NGC 315.....	E <sup>+</sup> :	...	69.3	-22.3	333 ± 50	569 ± 59	0.8	17, 18
NGC 1399.....	E1 pec	...	18.1	-20.9	308 ± 28	424 ± 46	0.5	17, 18
NGC 2434.....	E0-1	...	14.9	-19.3	212.6 ± 1.7	331 ± 42	0.8	17, 18
NGC 3193.....	E2	...	17.3	-19.5	209 ± 29	303 ± 25	0.4	17, 18
NGC 3379.....	E1	...	10.1	-19.8	202 ± 18	259 ± 23	0.6	17, 18
NGC 3640.....	E3	...	15.2	-19.7	177.2 ± 6.8	279.2 ± 8.7	0.2	17, 18
NGC 4168.....	E2	...	28.9	-20.2	182.4 ± 5.8	287 ± 21	0.4	17, 18
NGC 4278.....	E1-2	...	7.9	-18.5	250.7 ± 7.7	416 ± 13	0.1	13, 18
NGC 4374.....	E1	...	12.2	-20.4	280 ± 25	410 ± 31	0.3	17, 18
NGC 4472.....	E2	...	11.3	-20.9	279 ± 19	464 ± 36	0.2	17, 18
NGC 4486.....	E <sup>+</sup> 0-1 pec	...	15.5	-21.5	351 ± 19	507 ± 38	0.2	17, 18
NGC 4494.....	E1-2	...	17.0	-20.6	124 ± 17	261 ± 25	0.2	17, 18
NGC 4589.....	E2	...	28.9	-20.6	214 ± 30	333 ± 22	0.3	17, 18
NGC 4636.....	E0-1	...	10.3	-19.6	186 ± 22	341 ± 13	0.2	17, 18
NGC 5846.....	E0-1	...	21.8	-20.8	266 ± 23	338.3 ± 8.8	0.8	17, 18
NGC 6703.....	SA0 <sup>-</sup>	...	34.7	-20.7	171.6 ± 1.6	222 ± 29	1.0	17, 18
NGC 7145.....	E0	...	24.5	-19.9	133.1 ± 4.8	210 ± 31	0.8	17, 18
NGC 7192.....	E <sup>+</sup> :	...	36.8	-20.6	186 ± 17	270 ± 18	0.4	17, 18
NGC 7507.....	E0	...	21.6	-20.4	236 ± 15	399 ± 61	0.6	17, 18
NGC 7626.....	E pec:	...	48.6	-21.4	225 ± 22	401 ± 32	1.0	17, 18

NOTES.—Parameters of the final sample of galaxies. Col. (2): Morphological classification from RC3 for HSB and elliptical galaxies and from ESO-LV for LSB galaxies, except for ESO 534-G20 (NASA/IPAC Extragalactic Database). Col. (3): Disk inclination derived for spirals as  $\cos^2 i = (q^2 - q_0^2)/(1 - q_0^2)$ . The observed axial ratio  $q = a/b$  is taken from RC3 and ESO-LV for HSB and LSB galaxies, respectively, except for ESO 446-G17 (Palunas & Williams 2000), ESO 206-G14 (McGaugh et al. 2001), IC 724 (Rubin et al. 1985), and galaxies from Baes et al. (2003), for which we adopted their inclination. The intrinsic flattening  $q_0 = 0.11$  is assumed following Guthrie (1992). For elliptical galaxies with H I data, the inclination is taken from the papers listed in col. (9). Col. (4): Distance either from papers listed in col. (9) or derived as  $V_0/H_0$  with  $H_0 = 75 \text{ km s}^{-1} \text{ Mpc}^{-1}$  and  $V_0$  the systemic velocity corrected for the motion of the Sun with respect to the Local Group as in Sandage & Tammann (1981). Col. (5): Absolute total blue magnitude from  $B_T$  corrected for inclination and extinction from RC3 for HSB and elliptical galaxies and from ESO-LV for LSB galaxies. Col. (6): Central velocity dispersion of the spheroidal component. Col. (7): Galaxy circular velocity. Col. (8): Farthest observed radius of the ionized-gas velocity curve in units of  $R_{25}$ . Here  $R_{25}$  is from RC3 for HSB and elliptical galaxies and from ESO-LV for LSB galaxies. Col. (9): References.

REFERENCES.—(1) Baes et al. 2003; (2) original references can be found in Ferrarese 2002; (3) Corsini et al. 1999; (4) Vega Beltrán et al. 2001; (5) Pizzella et al. 2004b; (6) Corsini et al. 2003; (7) A. Pizzella et al. 2005, in preparation; (8) Kim et al. 1988; (9) Franx et al. 1994; (10) Jorgensen et al. 1995; (11) Schiminovich et al. 1995; (12) Beuing et al. 2002; (13) Barth et al. 2002; (14) Lees 1994; (15) Carollo et al. 1993; (16) Morganti et al. 1997; (17) Davies et al. 1987; (18) Kronawitter et al. 2000.

rotation curve. We therefore applied to this latter galaxy sample the same flatness criterion applied to our sample.

In summary, we have 23 galaxies (15 HSB and eight LSB galaxies) from our preliminary sample, 16 spiral galaxies (out of 38) from Ferrarese (2002), and nine spiral galaxies (out of 12) from Baes et al. (2003). It should be noted that the final sample of HSB galaxies includes 11 early-type objects with Hubble type ranging from S0 to Sab. On the other hand, the sample by Baes et al. (2003) and Ferrarese (2002) was constituted only by late-type spirals with Hubble type Sb or later (except for the Sa NGC 2844).

Finally, we considered a sample of 24 elliptical galaxies with a flat rotation curve and for which both  $V_c$  and  $\sigma_c$  are available from the literature. They include 19 objects studied by Kronawitter et al. (2000), who derived  $V_c$  by dynamical modeling, and five objects for which  $V_c$  is directly derived from the flat portion of their H I rotation curves. The addition of these last five elliptical galaxies is important, as it allows us to test against model-dependent biases in the  $V_c$ - $\sigma_c$  relation.

The  $V_c$  of NGC 4278 has been estimated from both the H I rotation curve (Lees 1994; at a distance from the center of 3.3  $R_{25}$ ) and dynamical models (Kronawitter et al. 2000; at a distance from the center of 0.1  $R_{25}$ ). The values are in agreement within 2  $\sigma$  error bars. For the further analysis we adopted

the H I  $V_c$ , which has been obtained at a larger distance from the center.

The values  $\sigma_c$  of all the elliptical galaxies have been corrected to the equivalent of an aperture of radius  $r_e/8$  following the prescriptions of Jorgensen et al. (1995). The effective radius  $r_e$  is taken from de Vaucouleurs et al. (1991, hereafter RC3).

The basic properties of the complete sample of 40 HSB disk galaxies, eight LSB spiral galaxies, and 24 elliptical galaxies are listed in Table 1, as well as their values of  $V_c$  and  $\sigma_c$ .

### 3. RESULTS AND DISCUSSION

The  $V_c$  and  $\sigma_c$  data points of the final sample of galaxies are plotted in Figure 2. We applied a linear regression analysis to the data by adopting the method of Akritas & Bershadsky (1996) for bivariate correlated errors and intrinsic scatter (BCES) both in the  $\log V_c$ - $\log \sigma_c$  and  $V_c$ - $\sigma_c$  plane. We did not include LSB galaxies in the analysis because they appear to follow a different  $V_c$ - $\sigma_c$  relation, as we discuss later.

Following Ferrarese (2002) and Baes et al. (2003), we fit the function  $\log V_c = \alpha \log \sigma_c + \beta$  to the data in the  $\log V_c$ - $\log \sigma_c$  plane. We find

$$\log V_c = (0.74 \pm 0.07) \log \sigma_c + (0.80 \pm 0.15), \quad (1)$$

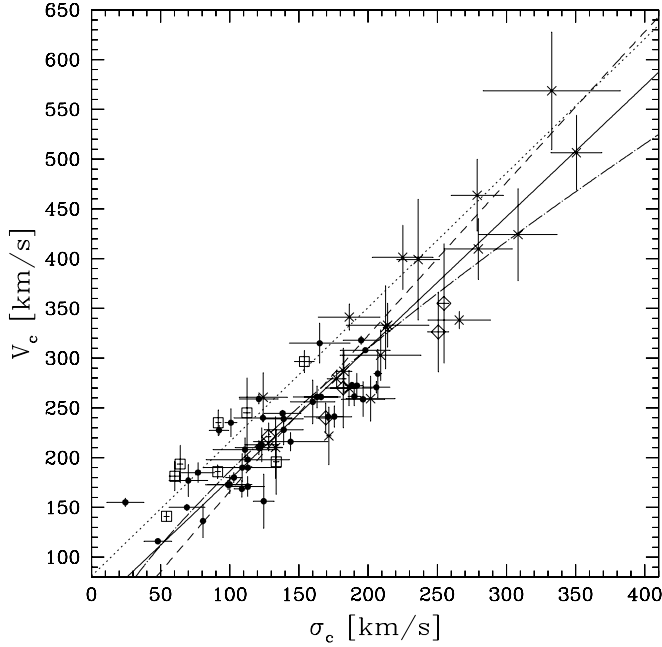


FIG. 2.—Correlation between the circular velocity  $V_c$  and the central velocity dispersion of the spheroidal component  $\sigma_c$  for elliptical and disk galaxies. The data points corresponding to HSB galaxies (*filled circles*), LSB galaxies (*squares*), elliptical galaxies with  $V_c$  obtained from H I data (*diamonds*), and elliptical galaxies with  $V_c$  obtained from dynamical models (*crosses*) are shown. The solid and dash-dotted lines represent the linear (eq. [3]) and power-law fits (eq. [1]) to HSB and elliptical galaxies. The dotted line represents the linear-law fit (eq. [8]) to LSB galaxies. The dashed line corresponds to the power-law fit to spiral galaxies with  $\sigma_c > 80 \text{ km s}^{-1}$  by Baes et al. (2003). [See the electronic edition of the Journal for a color version of this figure.]

with  $V_c$  and  $\sigma_c$  expressed in  $\text{km s}^{-1}$ . The resulting power law is plotted in Figure 2. To perform a comparison with previous results, we defined the reduced  $\chi^2$  as in Press et al. (1992),

$$\chi_v^2 = \frac{1}{N-2} \sum_{i=1}^N \frac{(\log V_{c,i} - \log V_{c,i}^{\text{fit}})^2}{\Delta \log V_{c,i}^2 + \alpha^2 \Delta \log \sigma_{c,i}^2}, \quad (2)$$

where  $\Delta \log \sigma_{c,i}$  and  $\Delta \log V_{c,i}$  are the errors of the  $i$ th data point,  $\log V_{c,i}$  and  $\log V_{c,i}^{\text{fit}}$  are the observed and fitted velocity of the  $i$ th data point,  $\alpha = 0.74$  is the linear coefficient of the regression, and  $N = 64$  is the number of data points. We find  $\chi_v^2 = 2.5$ .

The fitting power law has  $\alpha \approx 1$ , in agreement with Ferrarese (2002) and Baes et al. (2003). The power-law fit by Baes et al. (2003) is plotted in Figure 2 for comparison. However, Ferrarese (2002) and Baes et al. (2003) included in their fits only galaxies with  $\sigma_c > 70$  and  $\sigma_c > 80 \text{ km s}^{-1}$ , respectively. In fact, they considered the few objects with  $\sigma_c \leq 70 \text{ km s}^{-1}$  as outliers. On the other hand, we found that points characterized by  $\sigma_c \leq 70 \text{ km s}^{-1}$  appear to be well represented by the fitting law, as well as the ones characterized by higher values of  $\sigma_c$ .

Since it results that  $\alpha \approx 1$ , we decided to fit the function  $V_c = a\sigma_c + b$  to the data in the  $V_c$ - $\sigma_c$  plane. We find

$$V_c = (1.32 \pm 0.09)\sigma_c + (46 \pm 14), \quad (3)$$

with  $V_c$  and  $\sigma_c$  expressed in  $\text{km s}^{-1}$ . The resulting straight line is plotted in Figure 2. We find  $\chi_v^2 = 2.7$  by defining the reduced  $\chi^2$  as

$$\chi_v^2 = \frac{1}{N-2} \sum_{i=1}^N \frac{(V_{c,i} - V_{c,i}^{\text{fit}})^2}{\Delta V_{c,i}^2 + a^2 \Delta \sigma_{c,i}^2}, \quad (4)$$

where  $\Delta \sigma_{c,i}$  and  $\Delta V_{c,i}$  are the errors of the  $i$ th data point,  $V_{c,i}$  and  $V_{c,i}^{\text{fit}}$  are the observed and fitted velocity for  $i$ th data point,  $\alpha = 1.35$  is the linear coefficient of the regression, and  $N = 64$  is the number of data points.

To summarize, in previous works a power law was adopted to describe the correlation between  $V_c$  and  $\sigma_c$  for galaxies with  $\sigma_c > 80 \text{ km s}^{-1}$ . We find that data are also consistent with a linear law out to velocity dispersions as low as  $\sigma_c \approx 50 \text{ km s}^{-1}$ . We considered the straight line given in equation (3) as a reference fit.

Our reduced  $\chi^2$  is significantly higher than those found by Ferrarese (2002;  $\chi_v^2 = 0.5$  for a sample of 13 spiral galaxies with  $\sigma_c > 70 \text{ km s}^{-1}$  and 20 elliptical galaxies) and Baes et al. (2003;  $\chi_v^2 = 0.3$  for a sample of 24 spiral galaxies with  $\sigma_c > 80 \text{ km s}^{-1}$ ). However, this comparison is affected by the different uncertainties that characterize the  $V_c$  and  $\sigma_c$  measurements of the three data sets. In order to allow such a comparison, we performed an analysis of the scatter of the data points. We defined the scatter as

$$s = \sqrt{\frac{\sum_{i=1}^N d_i^2 w_i}{\sum_{i=1}^N w_i}}, \quad (5)$$

with

$$d_i = \frac{a\sigma_{c,i} - V_{c,i} + b}{\sqrt{a^2 + 1}}, \quad (6)$$

$$w_i = \frac{1}{\Delta \sigma_{c,i} \Delta V_{c,i}}, \quad (7)$$

where  $d_i$  and  $w_i$  are the distance between the  $i$ th data point and the straight line of coefficients  $a = 1.32$  and  $b = 46$  given in equation (3) and its weight, respectively. If we consider only the HSB galaxies, the resulting scatter is  $s = 11, 9,$  and  $23 \text{ km s}^{-1}$  for Ferrarese (2002), Baes et al. (2003), and our sample, respectively. The difference in the scatter of the data sets (e.g.,  $[s(\text{this work})/s(\text{Ferrarese})]^2 = 4.4$ ) is therefore significantly smaller than the difference of the corresponding  $\chi_v^2$  [e.g.,  $\chi_v^2(\text{this work})/\chi_v^2(\text{Ferrarese}) = 5.4$ ]. This means that the higher value of our  $\chi_v^2$  is mostly due to the smaller error bars, rather than to the larger intrinsic scatter of our HSB + elliptical data points. It should be noted that Ferrarese (2002) and Baes et al. (2003) considered only galaxies with a flat rotation curve extending at a distance  $R_{\text{last}}$  larger than the optical radius  $R_{25}$ . We relaxed this selection criterion to build our final sample and made sure instead that all rotation curves reached the flat outer parts. The residual plot of Figure 3 shows that the scatter of the data points corresponding to our sample galaxies with  $V_c$  measured at  $R_{\text{last}} \geq R_{25}$  is comparable to that of the galaxies with  $V_c$  measured at  $R_{\text{last}} < R_{25}$ . This confirms that this particular scale is not important once the asymptotic part of the rotation curve is reached by the observations. However, Figure 3 indicates that the residuals are particularly large near  $R_{\text{last}} \simeq R_{25}$  and that the scatter becomes smaller at  $R_{\text{last}} > 1.5R_{25}$ . In the latter case, the flat portion of the rotation curve extends on a

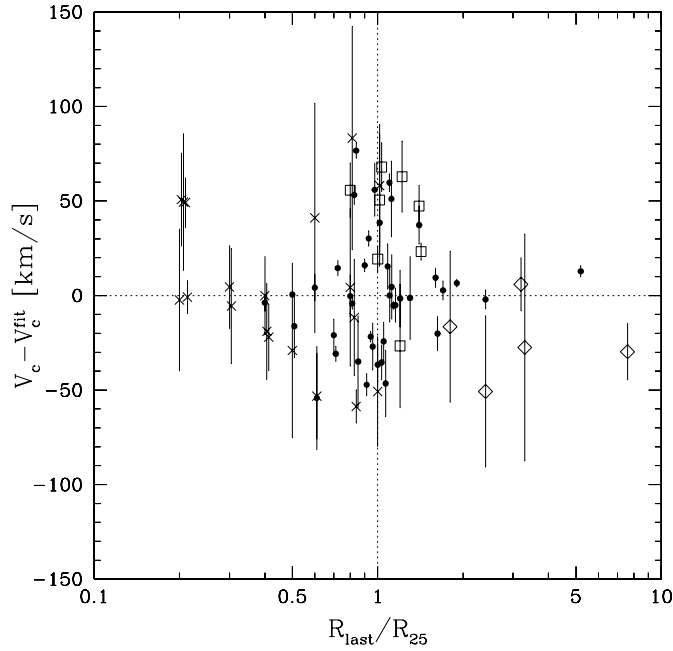


FIG. 3.—Residuals from the linear-law fit to HSB and elliptical galaxies (eq. [3]) plotted as function of  $R_{\text{last}}/R_{25}$ . The data points corresponding to HSB galaxies (filled circles), LSB galaxies (squares), elliptical galaxies with  $V_c$  obtained from H I data (diamonds), and elliptical galaxies with  $V_c$  obtained from dynamical models (crosses) are shown. Data with the same  $R_{\text{last}}/R_{25}$  have been shifted to allow comparison.

larger radial range, and therefore  $V_c$  is measured with a higher precision. In fact, for  $R_{\text{last}} \simeq R_{25}$  the scatter increases symmetrically with either  $V_c > V_{\text{fit}}$  or  $V_c < V_{\text{fit}}$  values, and this indicates that the less extended velocity curves are not introducing any systematic effect. Indeed, the slope of the  $V_c$ - $\sigma_c$  relation that we find is consistent with the one proposed by Ferrarese (2002) and Baes et al. (2003) from a sample of more extended velocity curves.

The measured scatter of the complete sample is  $s = 18 \text{ km s}^{-1}$ , which is larger than typical measurement errors for  $V_c$  and  $\sigma_c$  ( $\simeq 10 \text{ km s}^{-1}$ ). For this reason, the measured scatter is dominated by the intrinsic scatter, which we estimate to be  $\simeq 15 \text{ km s}^{-1}$ .

We investigated the location of the elliptical galaxies with  $V_c$  based on H I data and of LSB galaxies in the  $V_c$ - $\sigma_c$  plane. These types of galaxies were not considered by Ferrarese (2002) and Baes et al. (2003).

The data points corresponding to the five elliptical galaxies with  $V_c$  based on H I data follow the same relation as the remaining disk and elliptical galaxies. For these H I rotation curves we relaxed the flatness criterion in favor of their large radial extension, which is about 10 times larger than that of optical rotation curves. The inclusion of these data points does not change the fit based on the remaining disk and elliptical galaxies. They are mostly located on the upper end of the  $V_c$ - $\sigma_c$  relation derived for disk galaxies, in agreement with the findings of Bertola et al. (1993). They studied these elliptical galaxies and showed that their DM content and distribution are similar to those of spiral galaxies.

The LSB and HSB galaxies do not follow the same  $V_c$ - $\sigma_c$  relation. In fact, most of the LSB galaxies are characterized by a higher  $V_c$  for a given  $\sigma_c$  (or a lower  $\sigma_c$  for a given  $V_c$ ) with respect to HSB galaxies (Fig. 2). By applying to the LSB data points the same regression analysis that has been adopted

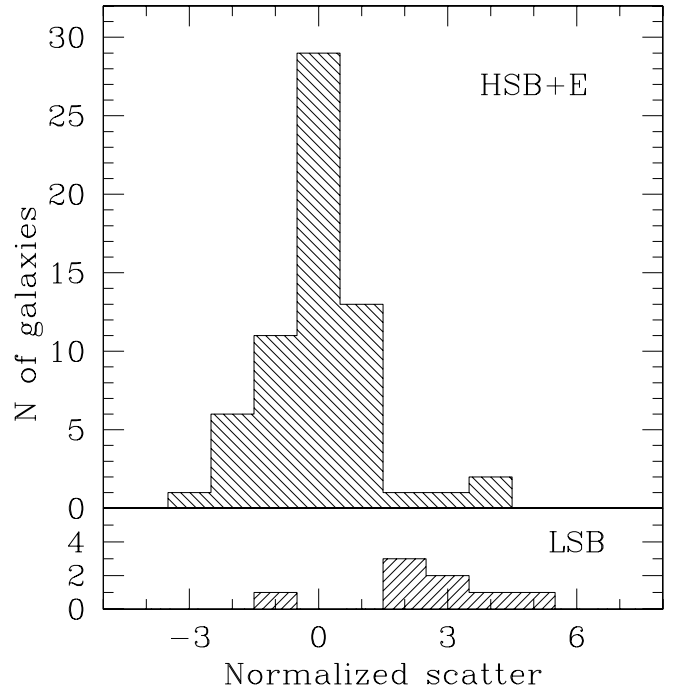


FIG. 4.—Distribution of the normalized scatter of the HSB and elliptical galaxies (top panel) and LSB galaxies (bottom panel) with respect to the linear-law fit to HSB and elliptical galaxies (eq. [3]). The two distributions are different at a  $>99\%$  confidence level.

for the HSB and elliptical galaxies of the final sample, we find

$$V_c = (1.35 \pm 0.19)\sigma_c + (81 \pm 23), \quad (8)$$

with  $V_c$  and  $\sigma_c$  expressed in  $\text{km s}^{-1}$ . The straight line corresponding to this fit, which is different from the one obtained for HSB and elliptical galaxies and happens to be parallel to it, is plotted in Figure 2.

To address the significance of this result, which is based only on eight data points, we compared the distribution of the normalized scatter of the LSB galaxies to that of the HSB and elliptical galaxies. We defined normalized scatter of the  $i$ th data point as

$$\bar{s}_i = d_i/\Delta_i, \quad (9)$$

where  $d_i$  is the distance to the straight line of coefficients  $a = 1.32$  and  $b = 46$  given in equation (3) of the  $i$ th data point, whose associated error  $\Delta_i$  is

$$\Delta_i = \sqrt{\Delta V_{c,i} \Delta \sigma_{c,i}}. \quad (10)$$

We assumed that  $\bar{s}_i > 0$  when the data point lies above the straight line corresponding to the best fit. In Figure 4 we plot the distributions of the normalized scatter of the LSB galaxies and of the HSB and elliptical galaxies. The two distributions appear to be different, as is confirmed at a high confidence level ( $>99\%$ ) by a Kolmogorov-Smirnov test. The fact that these objects fall in a different region of the  $V_c$ - $\sigma_c$  plane confirms that LSB and HSB galaxies constitute two different classes of galaxies.

Both demographics of supermassive black holes (SMBHs) and the study of DM distribution in galactic nuclei benefit from

the  $V_c$ - $\sigma_c$  relation. The recent finding that the mass of SMBHs correlates with different properties of the host spheroid supports the idea that formation and accretion of SMBHs are closely linked to the formation and evolution of their host galaxy. Such a mutual influence substantiates the notion of coevolution of galaxies and SMBHs (see Ho 2004).

A task to be pursued is to obtain a firm description of all these relationships spanning a wide range of SMBH masses and to address whether they hold for all Hubble types. In fact, the current demography of SMBHs suffers from important biases, related to the limited sampling over the different basic properties of their host galaxies. The finding that the  $V_c$ - $\sigma_c$  relation holds for small values of  $\sigma_c$  points to the idea that SMBHs with masses smaller than about  $10^6 M_\odot$  may also exist and follow the  $M_\bullet$ - $\sigma$  relation.

Moreover, it has been suggested that the  $V_c$ - $\sigma_c$  relation is equivalent to one between the masses of SMBHs and DM halos (Ferrarese & Merritt 2000; Baes et al. 2003), because  $\sigma_c$  and  $V_c$  are related to the masses of the central SMBH and DM halo, respectively. However, this claim is to be considered with caution, as the demography of SMBHs is still limited, in particular as far as spiral galaxies are concerned. Furthermore, the calculation of the virial mass of the DM halo from the measured  $V_c$  depends on the assumptions made for the DM density profile and the resulting rotation curve (e.g., see the prescriptions by Bullock et al. [2001] and Seljak [2002]). A better estimate of the virial velocity of the DM halo  $V_{\text{vir}}$  can be obtained by constraining the baryonic to dark matter fraction with detailed dynamical modeling of the sample galaxies. The resulting  $V_{\text{vir}}$ - $\sigma_c$  relation is expected to have a smaller scatter than the  $V_c$ - $\sigma_c$  relation. If the  $M_\bullet$ - $\sigma$  relation is to hold, then the deviation of LSB galaxies *with bulge* from the  $V_c$ - $\sigma_c$  relation of HSB and elliptical galaxies suggests that for a given DM halo mass the LSB gal-

axies would host a SMBH with a smaller mass compared to HSB galaxies. On the other hand, if the fundamental correlation of SMBH mass is with the halo circular velocity, then LSB galaxies should have larger black hole masses for a given bulge dispersion. The theoretical and numerical investigations of the processes leading to the formation of LSB galaxies thus should be accounted for.

The collapse of baryonic matter can induce a further concentration in the DM distribution (Rix et al. 1997) and a deepening of the overall gravitational well in the central regions. If this is the case, then the finding that at a given DM mass (as traced by  $V_c$ ) the central  $\sigma_c$  of LSB galaxies is smaller than in their HSB counterparts would argue against the relevance of baryon collapse in the radial density profile of DM in LSB galaxies. Confirming that LSB galaxies follow a different  $V_c$ - $\sigma_c$  relation will highlight yet another aspect of their different formation history. Indeed, LSB galaxies appear to have a central potential well less steep than HSB spirals of the same DM halo mass. If the collapse of baryonic matter causes a compression of the DM halo as well, for LSB galaxies such a process may have been less relevant than for HSB galaxies. Again, LSB galaxies turn out to be the best tracers of the primordial density profile of DM halos and therefore better for pursuing the nature of dark matter itself.

We are indebted to Matthew Bershady for providing us with the BCES code, which was used to analyze the data. We wish to thank Maarten Baes and Laura Ferrarese for stimulating discussion. This research has made use of the Lyon-Meudon Extragalactic Database (LEDA) and of the NASA/IPAC Extragalactic Database (NED).

## REFERENCES

- Akritas, M. G., & Bershady, M. A. 1996, *ApJ*, 470, 706  
 Baes, M., Buyle, P., Hau, G. K. T., & Dejonghe, H. 2003, *MNRAS*, 341, L44  
 Barth, A. J., Ho, L. C., & Sargent, W. L. W. 2002, *AJ*, 124, 2607  
 Beijersbergen, M., de Blok, W. J. G., & van der Hulst, J. M. 1999, *A&A*, 351, 903  
 Bertola, F., Cinzano, P., Corsini, E. M., Pizzella, A., Persic, M., & Salucci, P. 1996, *ApJ*, 458, L67  
 Bertola, F., Pizzella, A., Persic, M., & Salucci, P. 1993, *ApJ*, 416, L45  
 Beuing, J., Bender, R., Mendes de Oliveira, C., Thomas, D., & Maraston, C. 2002, *A&A*, 395, 431  
 Bullock, J. S., Kolatt, T. S., Sigad, Y., Somerville, R. S., Kravtsov, A. V., Klypin, A. A., Primack, J. R., & Dekel, A. 2001, *MNRAS*, 321, 559  
 Burstein, D., & Rubin, V. C. 1985, *ApJ*, 297, 423  
 Carollo, C. M., Danziger, I. J., & Buson, L. 1993, *MNRAS*, 265, 553  
 Corsini, E. M., Pizzella, A., Coccato, L., & Bertola, F. 2003, *A&A*, 408, 873  
 Corsini, E. M., et al. 1999, *A&A*, 342, 671  
 Davies, R. L., Burstein, D., Dressler, A., Faber, S. M., Lynden-Bell, D., Terlevich, R. J., & Wegner, G. 1987, *ApJS*, 64, 581  
 de Blok, W. J. G., & McGaugh, S. S. 1997, *MNRAS*, 290, 533  
 de Vaucouleurs, G., de Vaucouleurs, A., Corwin, H. G., Jr., Buta, R. J., Paturel, G., & Fouque, P. 1991, *Third Reference Catalogue of Bright Galaxies* (Berlin: Springer) (RC3)  
 Ferrarese, L. 2002, *ApJ*, 578, 90  
 Ferrarese, L., & Merritt, D. 2000, *ApJ*, 539, L9  
 Franx, M., van Gorkom, J. H., & de Zeeuw, T. 1994, *ApJ*, 436, 642  
 Gerhard, O., Kronawitter, A., Saglia, R. P., & Bender, R. 2001, *AJ*, 121, 1936  
 Guthrie, B. N. G. 1992, *A&AS*, 93, 255  
 Ho, L. C., ed. 2004, *Coevolution of Black Holes and Galaxies* (Cambridge: Cambridge Univ. Press)  
 Impey, C. D., Sprayberry, D., Irwin, M. J., & Bothun, G. D. 1996, *ApJS*, 105, 209  
 Jorgensen, I., Franx, M., & Kjaergaard, P. 1995, *MNRAS*, 276, 1341  
 Kim, D.-W., Jura, M., Guhathakurta, P., Knapp, G. R., & van Gorkom, J. H. 1988, *ApJ*, 330, 684  
 Kronawitter, A., Saglia, R. P., Gerhard, O., & Bender, R. 2000, *A&AS*, 144, 53  
 Lauberts, A., & Valentijn, E. A. 1989, *The Surface Photometry Catalogue of the ESO-Uppsala Galaxies* (Garching: ESO) (ESO-LV)  
 Lees, J. F. 1994, in *Mass-Transfer Induced Activity in Galaxies*, ed. I. Shlosman (Cambridge: Cambridge Univ. Press), 432  
 McGaugh, S. S., Rubin, V. C., & de Blok, W. J. G. 2001, *AJ*, 122, 2381  
 Morganti, R., Sadler, E. M., Oosterloo, T., Pizzella, A., & Bertola, F. 1997, *AJ*, 113, 937  
 Palunas, P., & Williams, T. B. 2000, *AJ*, 120, 2884  
 Persic, M., Salucci, P., & Stel, F. 1996, *MNRAS*, 281, 27  
 Pizzella, A., Corsini, E. M., Bertola, F., Coccato, L., Magorrian, J., Sarzi, M., & Funes, J. G. 2004a, in *IAU Symp. 220, Dark Matter in Galaxies*, ed. S. Ryder et al. (San Francisco: ASP), 337  
 Pizzella, A., Corsini, E. M., Vega Beltrán, J. C., & Bertola, F. 2004b, *A&A*, 424, 447  
 Press, W. H., Teukolsky, S. A., Vetterling, W. T., & Flannery, B. P. 1992, *Numerical Recipes in FORTRAN: The Art of Scientific Computing* (2nd ed.; Cambridge: Cambridge Univ. Press)  
 Rix, H., de Zeeuw, P. T., Cretton, N., van der Marel, R. P., & Carollo, C. M. 1997, *ApJ*, 488, 702  
 Rubin, V. C., Burstein, D., Ford, W. K., & Thonnard, N. 1985, *ApJ*, 289, 81  
 Sandage, A., & Tammann, G. A. 1981, *Carnegie Inst. Washington Publ.* 635, 0, 0  
 Schiminovich, D., van Gorkom, J. H., van der Hulst, J. M., & Malin, D. F. 1995, *ApJ*, 444, L77  
 Schombert, J. M., Bothun, G. D., Schneider, S. E., & McGaugh, S. S. 1992, *AJ*, 103, 1107  
 Seljak, U. 2002, *MNRAS*, 334, 797  
 Vega Beltrán, J. C., Pizzella, A., Corsini, E. M., Funes, J. G., Zeilinger, W. W., Beckman, J. E., & Bertola, F. 2001, *A&A*, 374, 394  
 Whitmore, B. C., & Kirshner, R. P. 1981, *ApJ*, 250, 43  
 Whitmore, B. C., Schechter, P. L., & Kirshner, R. P. 1979, *ApJ*, 234, 68